Diffusive structural colour in *Hoplia argentea*

Cédric Kilchoer [1], Primož Pirih [2], Ullrich Steiner [1] and Bodo D. Wilts [1*]

[1] *Adolphe Merkle Institute, University of Fribourg, Chemin des Verdiers 4, 1700 Fribourg, Switzerland*

[2] *Department of Biology, Biotechnical faculty, University of Ljubljana, Ljubljana, Slovenia*

*Author for correspondence: bodo.wilts@unifr.ch

Keywords: iridescence – insect colours – pigment filter – light scattering – camouflage

ORCID: 0000-0001-7453-4142 (CK); 0000-0003-1710-444X (PP)
0000-0001-5936-339X (US); 0000-0002-2727-7128 (BDW)

Abstract

Nature's nanostructures can bring about vivid and iridescent colours seen in many insects, notably in beetles and butterflies. While the intense structural colours can be advantageous for display purposes, they may be also appealing to predators and therefore constitute an evolutionary disadvantage. Animals often employ absorption and scattering in order to reduce the directionality of the reflected light and thereby enhance their camouflage. Here, we investigate the monkey beetle *Hoplia argentea* using microspectrophotometry, electron microscopy, fluorimetry and optical modelling. We show that the dull green dorsal colour comes from the nanostructured scales on the elytra. The nanostructure consists of a multi-layered photonic structure covered by a filamentous layer. The filamentous layer acts as a spatial diffuser of the specular reflection from the multilayer and suppresses the iridescence. This combination leads to a colour-stable and angle-independent green reflection that likely enhances the camouflage of the beetles in their natural habitat.

Background

Colouration in insects accomplishes a range of different functions, e.g. camouflage or signalling to mates and predators (Berthier, 2007; Doucet and Meadows, 2009; Howard, 2014; Hubbs, 1942). Pigmentary colour in insects is usually due to organic dyes in the sub-epidermal tissue, the integument, and the cuticle. Incident light that is not selectively absorbed by the pigments is isotropically scattered, resulting in dull, angle-independent colour. In contrast, some insects have structural colour that arises from the interaction of incident light with nanostructures in their scales (Srinivasarao, 1999). Periodic nanostructures produce vivid colours (Biró and Vigneron, 2011), which are strongly reflective, iridescent and specular (Doucet and Meadows, 2009). Structural colouration can be observed on butterfly wings scales, and on the cuticle and the scales of beetles (Seago et al., 2009; Stavenga et al., 2011a).

Colour is not only used for signalling. When it comes to camouflage, insects mimic the colouration of their environment to remain unnoticed to the eyes of potential predators (Stevens and Merilaita, 2011). Camouflage can be achieved either by spectrally adapting to the background (Schaefer and Stobbe, 2006), by transparency (Johnsen, 2001; Siddique et al., 2015; Yoshida et al., 1996), or by broadband reflectivity (Holt et al., 2011; Jordan et al., 2012; Vukusic et al., 2009; Wilts et al., 2013b). The main habitats of most insects - plants, soil and rocks - are generally diffusely reflecting and have reflectance spectra with broad peaks. The strong reflectivity and the colour change of iridescent structures may therefore be disadvantageous for efficient camouflage with these backgrounds. Many beetles and butterflies have evolved methods that suppress iridescence from structural colour by orientational averaging or spectral filtering (Wilts et al., 2012a; Wilts et al., 2012b).

A striking example of vivid beetle colouration is demonstrated by the well-investigated males of a monkey beetle species *Hoplia coerulea* (Coleoptera: Scarabaeidae: Hopliini) that possess a multilayered, porous nanostructure which produces a specular reflection with a reflectance peak of 0.6 at blue wavelengths with respect to a mirror (Mouchet et al., 2017; Vigneron et al., 2005). This striking colour is thought to be used to attract the females (Rassart et al., 2009). In recent years, *H. coerulea* received considerable attention because of its water vapour-sensitive optical properties (Mouchet et al., 2016a; Mouchet et al., 2016b). Many *Hoplia* species exists with little or no scales and a dull brown appearance due to the colour of the cuticle. Here, we investigate the colouration of the elytral scales of *H. argentea* (deprecated synonym *H.*

farinosa), a beetle commonly observed across Europe, which has the elytra covered by scales but has a more dull green appearance. In Alpine regions, such as Northern Slovenia and Switzerland, the abundance of *H. argentea* often reaches gregarious proportions in the period May-July. The adults inhabit wet places with lush vegetation and may be observed feeding and mating on plants with large inflorescences, e.g. elderberry, umbellifers, and plants from the rose family. The females lay their eggs to the ground, the larvae feed in the ground on rootlets (Brelih, S. ; Kajzer, A. ; Pirnat, 2010).

In contrast with the sexually strongly dimorphic *H. coerulea*, for which the elytra of males are shiny blue, both sexes of *H. argentea* are dull green and less conspicuous from the vegetation background. This difference was pointed out by Gentil in 1943 in the first attempt to compare the scale ultrastructure of both species (Gentil, 1943). The origin of the structural colouration was not fully characterized at the time. Here, we show that the colouration of *H. argentea*'s dorsal side results from combining a porous chitin/air multilayer reflector with absorptive filtering and scattering by a brush-like, diffusive layer on the upper (adwing) side of the scales. We discuss the possible function of shedding the scales, which brings about the hue change from green to brown. This change might be an adaptive camouflage mechanism for females that lay the eggs on the ground.

Material and Methods

Specimen

Specimen of *Hoplia argentea* (Poda, 1761) were captured around Évolène (Switzerland, N =2) and around Jezersko and Ilirska Bistrica (both Slovenia, N = 5) in June and July 2019. Samples were stored in dry (RH < 25 %) and dark conditions before the measurements that were performed in lab conditions.

Optical characterization

Spectral characterization was performed using a xenon light source (Thorlabs SLS401; Thorlabs GmbH, Dachau, Germany) and a ZEISS Axio Scope.A1 microscope (Zeiss AG, Oberkochen, Germany). The light reflected from the sample was collected using an optical fibre (QP230-2-XSR, 230 µm core) with a measurement spot size of approximately 10 µm and a protected silver mirror (Thorlabs PF10-03-P01) was used as a reference. The spectra were recorded by a spectrometer (Ocean Optics Maya2000 Pro; Ocean Optics, Dunedin, FL, USA). Optical micrographs were captured with a CCD camera (GS3-U3-28S5C-C, Point Grey/ FLIR

Integrated Imaging Solutions Inc., Richmond, Canada). Measurements of the far-field reflection were accessed by placing a Bertrand lens (Zeiss 453671) in the imaging pathway, using a high numerical aperture air objective (Zeiss Epiplan Neofluar 50x, NA 0.95)

Fluorescence characterization

Fluorescence images were acquired using a DP72 Colour CCD Camera mounted on a BX51 microscope (all Olympus Corporation, Tokyo, Japan). The excitation/filtering wavelengths for the blue, green and red channels were 330-380/420 nm, 450-480/515 nm, and 510-550/590 nm, respectively. Samples were illuminated using a mercury lamp (X-Cite 120Q, Excelitas Technologies Corp., Waltham, MA, USA).

Spectrofluorimetry experiments were performed on parts of the elytrae, using a Horiba Fluorolog system (Horiba Scientific, Kyoto, Japan). The measurements were performed with a 4 nm bandpass slit for the excitation and a 3 nm bandpass slit for the emission, with 0.1 s integration time. The incident light formed a 30° angle with the sample normal. The emitted light was detected at a 60° normal angle.

Scanning electron microscopy (SEM)

A wing piece was cut from the beetle and glued onto a standard SEM stub. The sample was imaged using a FEI Scios 2 dual-beam field-emission electron microscope (FEI, Eindhoven, the Netherlands). To prevent charging effects, a 5 nm gold layer was sputtered on the sample using a Cressington (Cressington Scientific Instruments, Watford, England) 208 HR sputter coater.

Optical modelling

The optical simulation was carried out using the transfer-matrix method (Yeh, 2005). The simulated system had 6 bilayers consisting of a 110±30 nm porous chitin layer and a 95±30 nm solid chitin layer, as estimated from morphological data (standard deviation). To mimic natural variations, the thickness of each layer in the simulation was taken from this interval. The refractive index used for porous and solid chitin layers was assumed to be 1.10 and 1.55, respectively. The refractive index of the porous layer is slightly above the refractive index of air, $n = 1.00$, in order to account for the filling factor of chitin in the porous layers. In order to account for the layer thickness variation, the reflectance spectrum simulation was repeated 100 times and averaged.

Results

Optical appearance and anatomy

H. argentea beetles have a typical body length of around 1 cm (Figure 1A), with an overall dull-green colour on the dorsal side. A closer look of the elytron revealed that a red-brown to black-brown cuticle is covered by green-coloured scales (Figure 1B). The scales typically have a rounded shape with a diameter of 50±10 µm and lay on the elytron in a single layer (Figure 1C). The reflection of individual scales and the elytron was spectrally characterized using a custom-built microspectrophotometer. The black-brown elytron has a spectrally flat reflectance below ~0.05 at visible wavelengths, indicative of the presence of a broadband-absorbing pigment, likely melanin. In contrast, the green scales exhibit a pronounced reflection peak at ~540 nm with a full width at half maximum of ~100 nm (Figure 1D). The dull green colouration of the beetle arises mostly due to the reflection from the scales. Some animals lose their scales through wear (likely caused by frequent mounting during mating attempts), resulting in a change of the overall hue from dull green to brown (Figure S3). The iridescent colour of the ventral side of the animals seems to be more consistent among specimens and is due to blue-green, specularly reflecting scales (Figure S4).

Scale anatomy: pigments and multilayers

To understand the basis of the colour, we investigated the scale anatomy and the presence of pigments. First, a refractive index-matching experiment was conducted to establish the presence of absorbing pigments within the scales (Stavenga et al., 2013). The transmission spectrum of a single scale was recorded in air and immersed in a refractive index fluid of $n = 1.55$ (Figure S1). The transmittance drastically increased at long wavelengths since interfacial scattering was removed by the index-matching fluid, while the presence of a UV-absorbing pigment with increasing absorbance towards the UV (<400 nm) became apparent.

The UV-absorbing pigment is fluorescent (Figures S2). This allowed imaging of the wing scales (Figure 2A) using fluorescence microscopy (Figure 2B) to determine the pigment distribution throughout the scale. The scale in cross-section has a two-tiered structure. The upper, abwing layer contains short filaments. The lower, adwing layer appears solid. The fluorophore can be detected in both tiers, but is predominantly present in the lower layer.

To better resolve the scale ultrastructure, scanning electron microscopy was employed. The top-view of a single scale shows a brush-like structure with hundreds of small filaments with a diameter of 480±50 nm and a length of ~5 µm (Figure 2C) that are also visible in the fluorescence micrograph of Figure 2D. The filaments are rather disorderly arranged on the scale and do not show a common orientation. The density is estimated at 65±7 filaments per 10 x 10 μm^2.

To visualise the optical structure below the filamentous brush, a single scale was sectioned with a focussed-ion beam. The scale cross-section in Figure 2E shows that the ultrastructure is composed of two distinct parts. A filamentous top layer covers a photonic structure consisting of alternating layers of solid and macroporous chitin with thicknesses of 95±30 nm and 110±30 nm, respectively. The structure of the photonic multilayer appear to be similar to that observed in the related *H. coerulea* (Mouchet et al., 2016a; Rassart et al., 2009; Vigneron et al., 2005).

Spectral averaging and camouflage

To understand the influence of the scale anatomy on the optical properties, the spatial reflection patterns from single scales were spectrally characterized using a microspectrophotometer (Figure 3). We illuminated the scale from the abwing side (filaments first) and adwing side (multilayer first), Figure 3G. The angular distribution of the reflected and scattered light was characterized in the far-field, using a Bertrand lens. Under narrow-aperture illumination, the specularity of reflected light was investigated. When illuminated from the abwing side (Figure 3A), the reflected light is uniformly scattered to all angles (Figure 3B), indicating a diffuse reflection. When illuminated from the adwing side, the reflection was highly specular (Figure 3D,E), indicating that the adwing side of the scale is reflecting the light in a manner similar to a mirror. Under wide-aperture illumination, the light reflected from the abwing (Figure 3A) was chromatically uniform at all angles (Figure 3C), while the reflection from the adwing side showed that the reflection was varying from green at normal incidence to blue high incidence angles, typical of iridescence due to a multilayer structure (Figure 3F)

The reflectance of a single scale was spectrally characterized using a spectrometer coupled to a microscope, using epi-illumination from the abwing (filament side) and adwing (multilayer side) sides (Figure 3G). While the spectral shape was similar, the peak reflectance was ~0.2 and ~0.5 for the abwing and adwing side, respectively (Figure 3H). For comparison, a typical reflection from a green leaf peaks at around 550 nm, with peak reflectance of ~0.15,

comparable to the abwing reflection. We modelled the reflectance using a common multilayer model (Stavenga et al., 2011a) with the material parameters obtained from ultrastructure. The modelled spectrum (dotted line in Figure 3H) approximated well the measured reflectance of the adwing side.

Discussion

Diffusive reflection in *H. argentea*

The dull green colour of *H. argentea* results from a combination of a multilayer structure, an absorbing pigment and a filamentous diffuser. The ultrastructure of the scale is composed of two parts where a disordered brush-like layer overlays a periodic multilayer structure. This brush-like layer diffuses the light incident onto and reflected by the multilayer structure into the whole hemisphere. This eliminates the iridescence that is native to a periodic multilayer structure, thereby supressing the blue-shift at non-normal incidence or reflection angles as seen in the adwing scatterogram in Figure 3F. This results in a spectral and spatial reflectance pattern of the beetle elytra being similar to that of plant leaves (Figure 3H).

The addition of the filamentous layer to the beetle scale has a dramatic effect on the optical appearance of the *H. argentea* when compared to the brilliant blue-coloured *H. coerulea* (Gentil, 1943; Vigneron et al., 2005). It is noteworthy that the fluorescent pigmentation (see Figures 2bd, S2; c.f. (Mouchet et al., 2016c; Mouchet et al., 2019)) and the photonic structures are very similar in both beetles, with a slightly increased layer-to-layer distance in *H. argentea* (195 nm) compared to *H. coerulea* (175 nm) (Mouchet et al., 2016b; Rassart et al., 2009), resulting in reflection peaks in the green and blue, respectively. This suggests that the fabrication of the photonic structure is evolutionary adaptable. We have not explored the change of colour due to wetting in *H. argentea*, but it likely also present due to a similar porous structure as in *H. coerulea*. In the future, it may be worthwhile to explore whether the wetting might cause the apparent diversity of the dorsal colouration (between green and yellow), and whether the colour change has any influence on the intraspecific recognition (Briscoe and Chittka, 2001).

Camouflage by spectral filtering

The intensity and the uniform scattering of light reflected from *H. argentea* scales resemble the chlorophyll-based pigment reflection of green leaves in the part of the spectrum relevant for vision (320 to 650 nm; see Figures 1a, 3H). To mimic plant reflection, *H. argentea* combines a spectrally-selective, directional reflector with a pigment absorber and a diffuser in the scale ultrastructure. This suggests a function in camouflage, a commonly used survival strategy where animals try to reduce their visibility by mimicking the colouration of their environment. *Hoplia argentea* is not the first insect found to be using a photonic strategy to hide in a foliacious background. Many insects have employed similar strategies to decrease the iridescence of a photonic structure and to achieve a reflectance very close to that of chlorophyll-based plants. For example, some butterflies combine a gyroid photonic crystal with a pigmentary attenuation and spatial filtering (Wilts et al., 2012b; Wilts et al., 2017). Between their lower and upper lamina, the wing scales of *Parides* butterflies have a gyroid nanostructure acting as a selective reflector for green colour (Wilts et al., 2017). The reflected green light is filtered when it passes through a thick upper lamina that contains pigments. Quite similar to the beetle scales described here, this stacking results in spatial distribution of the reflection that is almost angle-independent. A combination of pigments and structural reflection is also present in green feathers of some parrots (Stavenga et al., 2011b) and budgerigars (D'Alba et al., 2012). Stable colouration by complex photonic morphologies has also been observed in dragonflies (Nixon et al., 2015), where a wrinkled multilayer spreads the reflected signal to a large angular range.

Other strategies are based on the nanostructures alone, where the dimensions of the ordered nanostructure plays an important role. As an example, the long-range order of diamond photonic crystals has been investigated in weevils (Nagi et al., 2018; Wilts et al., 2013a). In contrast to the highly specular reflection arising from a long-range ordered structure in *Entimus imperialis*, *Eupholus cuvieri* possesses multiple structural domains within the same scale. Those domains have different orientations, resulting in colour mixing and a rather diffuse green reflection (Wilts et al., 2013a), which facilitates camouflage.

Biological significance of the coloration

In *Hoplia coerulea*, the ventral sides of both sexes are covered with bright scales, while the dorsal sides are strongly dimorphic: the males have specular blue elytra, while the females are dull brown (Rassart et al., 2009). In contrast, the *Hoplia argentea* investigated here does not show a sexual dimorphism as both sexes have dull green to orange dorsal colour, while the ventral colour is blue-green iridescent. Dimorphism in monkey beetles was so far thought to be associated with day-active, flower visiting taxa where the colouration is supposed to serve display and mimicry (Ahrens et al., 2011). Our results add camouflage as yet another possible function. To that end, it is interesting that two related species found in Europe, *H. coerulea* and *H. argentea*, with seemingly similar ecology in terms of dwelling on the flowers, have evolved diverse colouration strategies and strong difference in dimorphism.

Further, we were surprised by the observation that the ventral, blue-green colour (Fig. S3) seems to be more consistent over the life time of a beetle than the dorsal colour, as the ventral scales seem to shed less than the dorsal scales (Fig. S4). The colour of the dorsal side therefore seems to be somewhat variable (with small shifts in the peak wavelength) in this species and we can list three possible contributing factors leading to this: (i) the scales may have slightly different structural properties among individuals (similar to differences between *H. coerulea* and *H. argentea*); (ii) the colour is influenced by humidity-dependent wetting, and (iii) the overall hue changes from green towards brown due to shedding ofscales from the elytra. Pending further studies, we hypothesise that this colour change may actually be beneficial to the survival of females as they progress from dwelling on the plants, where they feed and mate, to laying the eggs on soil.

Conclusion

In conclusion, the colouration mechanism in the green-coloured scales of *H. argentea* has been characterized. To achieve an angle-independent green reflection, the scale ultrastructure combines a multilayer photonic crystal below with a disordered layer of hair-like filaments. The reflected colour is mainly determined by the photonic crystal and then scattered by passing through the filament layer where it is scattered. This results in light reflection with a homogeneous angular distribution, mimicking common leaf colouration, thereby providing an

efficient camouflage strategy. Further, the species of the genus *Hoplia* seem to be employing different colouration strategies, and these differences may be related to their different life styles.

Additional statements.

Author contributions. CK collected specimen, performed experiments, analysed measurements, and wrote the manuscript. PP collected specimen and performed experiments. US wrote the manuscript. BDW performed experiments, wrote the manuscript and supervised the project. All authors gave final approval for publication.

Competing interests. The authors declare no competing or financial interests.

Data accessibility. All data is included within this manuscript and its supplementary information.

Acknowledgments. We gratefully thank Felipe Saenz for his help for the fluorimetry experiment, Gregor Belušič for supplying the animals and Al Vrezec for discussions on the species biology and for supplying the taxonomic literature. We are grateful to Pierre-Paul Bitton and the other anonymous reviewer(s) for useful comments on the manuscript.

Funding. This study was supported by the Swiss National Science Foundation through project grant 163220 (to US), Ambizione programme grant 168223 (to BDW), and the National Center of Competence in Research *Bio-inspired Materials*. This study was supported by the infrastructural centre for Microscopy of biological samples at Biotechnical faculty, University of Ljubljana.

References

Ahrens, D., Scott, M. and Vogler, A. P. (2011). The phylogeny of monkey beetles based on mitochondrial and ribosomal RNA genes (Coleoptera: Scarabaeidae: Hopliini). *Mol. Phylogenet. Evol.* **60**, 408–415.

Berthier, S. (2007). *Iridescences*. New York, NY: Springer New York.

Biró, L. P. and Vigneron, J. P. (2011). Photonic nanoarchitectures in butterflies and beetles: valuable sources for bioinspiration. *Laser Photon. Rev.* **5**, 27–51.

Brelih, S. ; Kajzer, A. ; Pirnat, A. (2010). Material for the beetle fauna (Coleoptera) of Slovenia 4th contribution: Polyphaga: Scarabaeoidea (=Lamellicornia). *Scopolia* **70**, 1–386.

Briscoe, A. D. and Chittka, L. (2001). The evolution of color vision in insects. *Annu. Rev. Entomol.* **46**, 471–510.

D'Alba, L., Kieffer, L. and Shawkey, M. D. (2012). Relative contributions of pigments and biophotonic nanostructures to natural color production: a case study in budgerigar (*Melopsittacus undulatus*) feathers. *J. Exp. Biol.* **215**, 1272–1277.

Doucet, S. M. and Meadows, M. G. (2009). Iridescence: a functional perspective. *J. R. Soc. Interface* **6**, S115–S132.

Gentil, K. (1943). Beitrag zur morphologie und optik der schillerschuppen von *Hoplia coerulea* Drury und *Hoplia farinosa* Linné (col.). *Zeitschrift für Morphol. und Ökologie der Tiere* **40**, 299–313.

Holt, A. L., Sweeney, A. M., Johnsen, S. and Morse, D. E. (2011). A highly distributed Bragg stack with unique geometry provides effective camouflage for Loliginid squid eyes. *J. R. Soc. Interface* **8**, 1386–1399.

Howard, R. (2014). Principles of Animal Communication. *Am. Entomol.* **45**, 126–126.

Hubbs, C. L. (1942). Adaptive Coloration of Animals. *Am. Nat.* **76**, 500.

Johnsen, S. (2001). Hidden in plain sight: the ecology and physiology of organismal transparency. *Biol. Bull.* **201**, 301–18.

Jordan, T. M., Partridge, J. C. and Roberts, N. W. (2012). Non-polarizing broadband multilayer reflectors in fish. *Nat. Photonics* **6**, 759–763.

Mouchet, S. R., Van Hooijdonk, E., Welch, V. L., Louette, P., Colomer, J.-F., Su, B.-L. and Deparis, O. (2016a). Liquid-induced colour change in a beetle: the concept of a photonic cell. *Sci. Rep.* **6**, 19322.

Mouchet, S. R., Tabarrant, T., Lucas, S., Su, B.-L., Vukusic, P. and Deparis, O. (2016b). Vapor sensing with a natural photonic cell. *Opt. Express* **24**, 12267.

Mouchet, S. R., Lobet, M., Kolaric, B., Kaczmarek, A. M., Van Deun, R., Vukusic, P., Deparis, O. and Van Hooijdonk, E. (2016c). Controlled fluorescence in a beetle's photonic structure and its sensitivity to environmentally induced changes. *Proc. R. Soc. B: Biol. Sci.* **283**, 20162334.

Mouchet, S. R., Lobet, M., Kolaric, B., Kaczmarek, A. M., Van Deun, R., Vukusic, P., Deparis, O. and Van Hooijdonk, E. (2017). Photonic scales of *Hoplia coerulea* beetle: Any colour you like. In *Materials Today: Proceedings*, pp. 4979–4986.

Mouchet, S. R., Verstraete, C., Mara, D., Van Cleuvenbergen, S., Finlayson, E. D., Van Deun, R., Deparis, O., Verbiest, T., Maes, B., Vukusic, P., et al. (2019). Nonlinear optical spectroscopy and two-photon excited fluorescence spectroscopy reveal the excited states of fluorophores embedded in a beetle's elytra. *Interface Focus* **9**, 20180052.

Nagi, R. K., Montanari, D. E. and Bartl, M. H. (2018). Photonic crystal micro-pixelation and additive color mixing in weevil scales. *Bioinspir. Biomim.* **13**, 035003.

Nixon, M. R., Orr, A. G. and Vukusic, P. (2015). Wrinkles enhance the diffuse reflection from the dragonfly *Rhyothemis resplendens*. *J. R. Soc. Interface* **12**, 20140749.

Rassart, M., Simonis, P., Bay, A., Deparis, O. and Vigneron, J. P. (2009). Scale coloration change following water absorption in the beetle *Hoplia coerulea* (Coleoptera). *Phys. Rev. E - Stat. Nonlinear, Soft Matter Phys.* **80**, 031910.

Schaefer, H. M. and Stobbe, N. (2006). Disruptive coloration provides camouflage independent of background matching. *Proc. R. Soc. B: Biol. Sci.* **273**, 2427–2432.

Seago, A. E., Brady, P., Vigneron, J.-P. and Schultz, T. D. (2009). Gold bugs and beyond: a review of iridescence and structural colour mechanisms in beetles (Coleoptera). *J. R. Soc. Interface* **6**, S165–S184.

Siddique, R. H., Gomard, G. and Hölscher, H. (2015). The role of random nanostructures for the omnidirectional anti-reflection properties of the glasswing butterfly. *Nat. Commun.* **6**, 6909.

Srinivasarao, M. (1999). Nano-Optics in the Biological World: Beetles, Butterflies, Birds, and Moths. *Chem. Rev.* **99**, 1935–1962.

Stavenga, D. G., Wilts, B. D., Leertouwer, H. L. and Hariyama, T. (2011a). Polarized iridescence of the multilayered elytra of the Japanese jewel beetle, *Chrysochroa fulgidissima*. *Philos. Trans. R. Soc. B Biol. Sci.* **366**, 709–723.

Stavenga, D. G., Tinbergen, J., Leertouwer, H. L. and Wilts, B. D. (2011b). Kingfisher feathers - colouration by pigments, spongy nanostructures and thin films. *J. Exp. Biol.* **214**, 3960–3967.

Stavenga, D. G., Leertouwer, H. L. and Wilts, B. D. (2013). Quantifying the refractive index dispersion of a pigmented biological tissue using Jamin-Lebedeff interference microscopy. *Light Sci. Appl.* **2**, e100.

Stevens, M. and Merilaita, S. (2011). *Animal camouflage*. (ed. Stevens, M.) and Merilaita, S.) Cambridge: Cambridge University Press.

Vigneron, J. P., Colomer, J. F., Vigneron, N. and Lousse, V. (2005). Natural layer-by-layer photonic structure in the squamae of *Hoplia coerulea* (Coleoptera). *Phys. Rev. E - Stat. Nonlinear, Soft Matter Phys.* **72**, 061904.

Vukusic, P., Kelly, R. and Hooper, I. (2009). A biological sub-micron thickness optical broadband reflector characterized using both light and microwaves. *J. R. Soc. Interface* **6**,.

Wilts, B. D., Trzeciak, T. M., Vukusic, P. and Stavenga, D. G. (2012a). Papiliochrome II pigment reduces the angle dependency of structural wing colouration in *nireus* group papilionids. *J. Exp. Biol.* **215**, 796–805.

Wilts, B. D., Michielsen, K., De Raedt, H. and Stavenga, D. G. (2012b). Iridescence and spectral filtering of the gyroid-type photonic crystals in *Parides sesostris* wing scales. *Interface Focus* **2**, 681–687.

Wilts, B. D., Ijbema, N., Michielsen, K., De Raedt, H. and Stavenga, D. G. (2013a). Shine and hide: Biological photonic crystals on the wings of weevils. In *Materials Research Society Symposium Proceedings*, pp. 1–6.

Wilts, B. D., Pirih, P., Arikawa, K. and Stavenga, D. G. (2013b). Shiny wing scales cause spec(tac)ular camouflage of the angled sunbeam butterfly, *Curetis acuta*. *Biol. J. Linn. Soc.* **109**, 279–289.

Wilts, B. D., Apeleo Zubiri, B., Klatt, M. A., Butz, B., Fischer, M. G., Kelly, S. T., Spiecker, E., Steiner, U. and Schröder-Turk, G. E. (2017). Butterfly gyroid nanostructures as a time-frozen glimpse of intracellular membrane development. *Sci. Adv.* **3**, e1603119.

Yeh, P. (2005). *Optical waves in layered media*. Hoboken, NJ: Wiley.

Yoshida, A., Motoyama, M., Kosaku, A. and Miyamoto, K. (1996). Nanoprotuberance Array in the Transparent Wing of a Hawkmoth, *Cephonodes hylas*. *Zoolog. Sci.* **13**, 525–526.

Figures

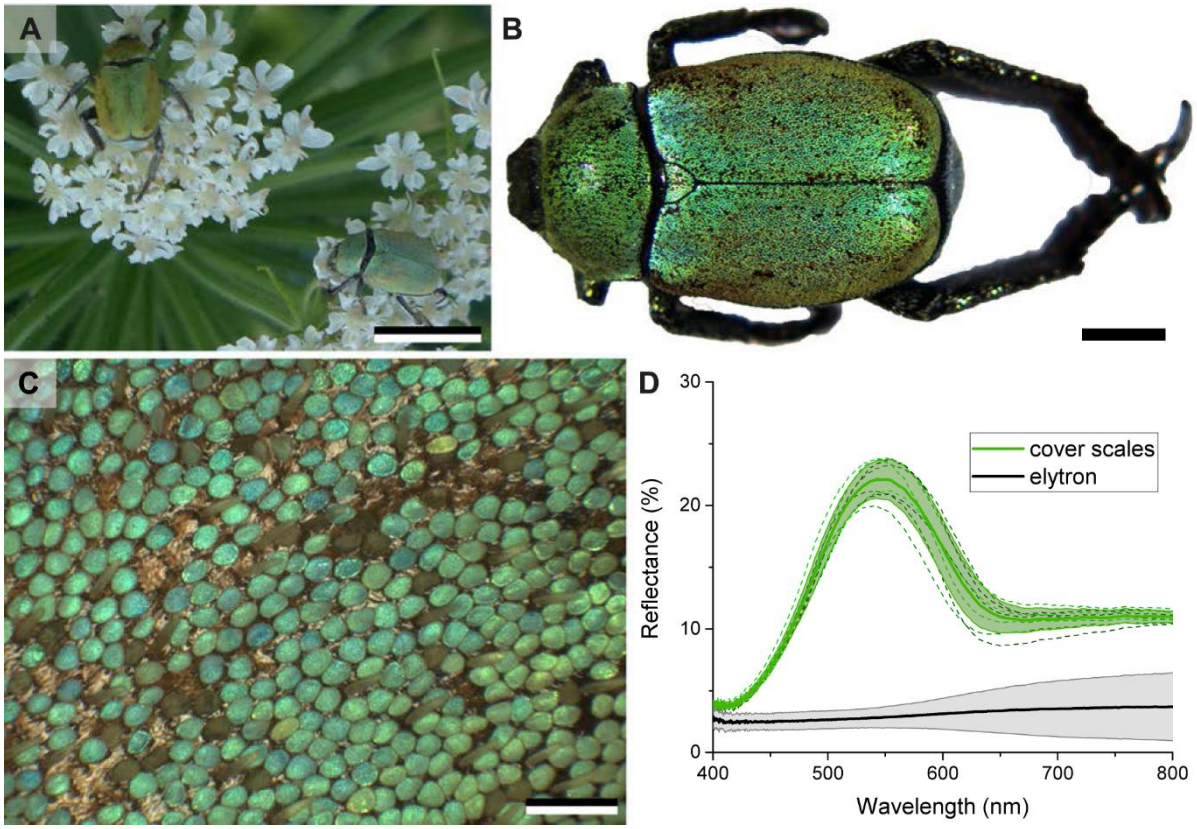

Figure 1. ***Hoplia argentea.*** A) Specimen in their natural habitat. B) Close-up photograph of a specimen with black-brown cuticle and many scales. C) Optical micrograph of the beetle elytron. D) Reflection of the beetle scales (green) and elytron (black). For cover scales, the dashed lines show reflectance spectra from individual scales. The bands show the mean ± s.d. of the reflectance spectrum (N = 10 scales, N = 5 elytron). Scale bars: (A) 10 mm, (B) 2 mm, (C) 200 µm.

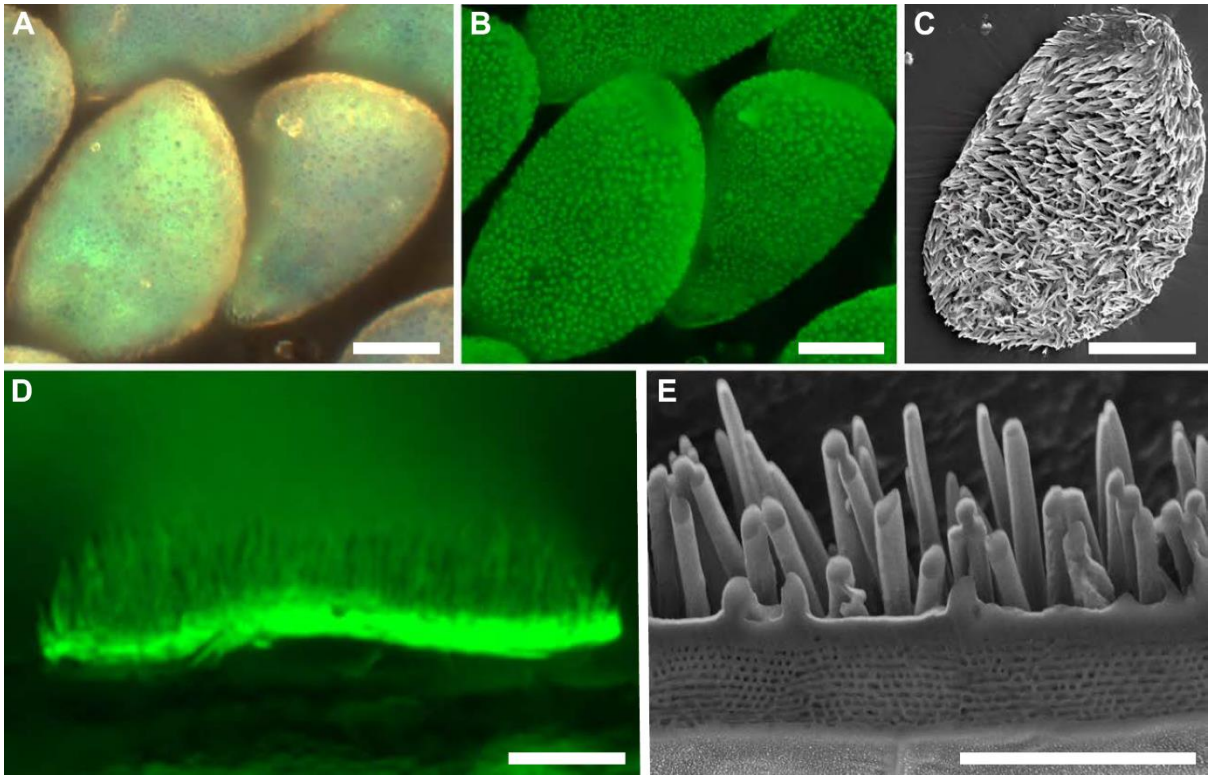

Figure 2. Scale ultrastructure and fluorescence. A) Epi-illumination micrograph of the beetle's elytra scales. B) Fluorescence micrograph of the same scales. C) Top-view scanning electron micrograph of a single scale. The scale is covered by brush-like filaments. D) Cross-sectional view of the scale in fluorescence microscopy. The source of fluorescence is mostly located in the scale base. E) FIB-SEM imaging of a scale cross-section. The scale ultrastructure is composed of a porous multilayer photonic crystal below the filament layer on the abwing side. The excitation/filtering wavelengths for the green fluorescence microscopy (B, D) are 450-480/515 (see also Fig. S2). Scale bars: (A, B, C) 20 µm, (D, E) 5 µm.

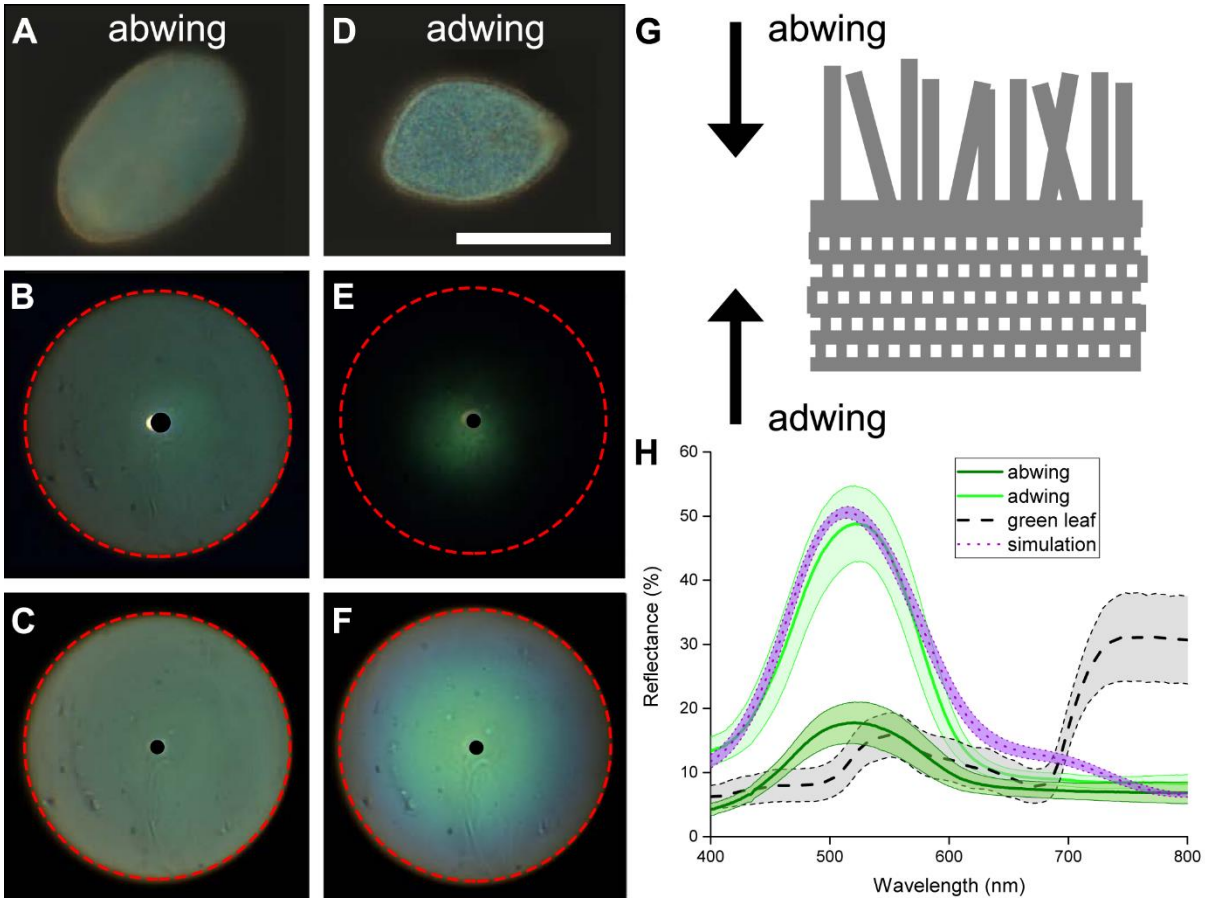

Figure 3. *k*-space imaging and reflectance spectra of *H. argentea* scales from the abwing (A, B, C) and adwing (D, E, F) side. *k*-space imaging was performed under narrow (B, E) and wide aperture illumination (C ,F). The red dashed circle represents the aperture of the objective, corresponding to the scattering angle ~71°. Scale bar: 50 µm. (G) Schematic representation of the scale. Dark arrows represent the direction of the incoming light for ab- and adwing measurements. The reflection of the different sides compared to a green leaf is depicted in (H). Solid lines represent experimental measurement of ab- and adwing scales (N = 9, 8 respectively). The dashed line is the reflection of a green leaf (N = 10). The dotted purple line is a simulated reflectance spectrum of a multilayer photonic crystal without diffusive elements (all curves show mean ± s.d.).

Supplementary Information

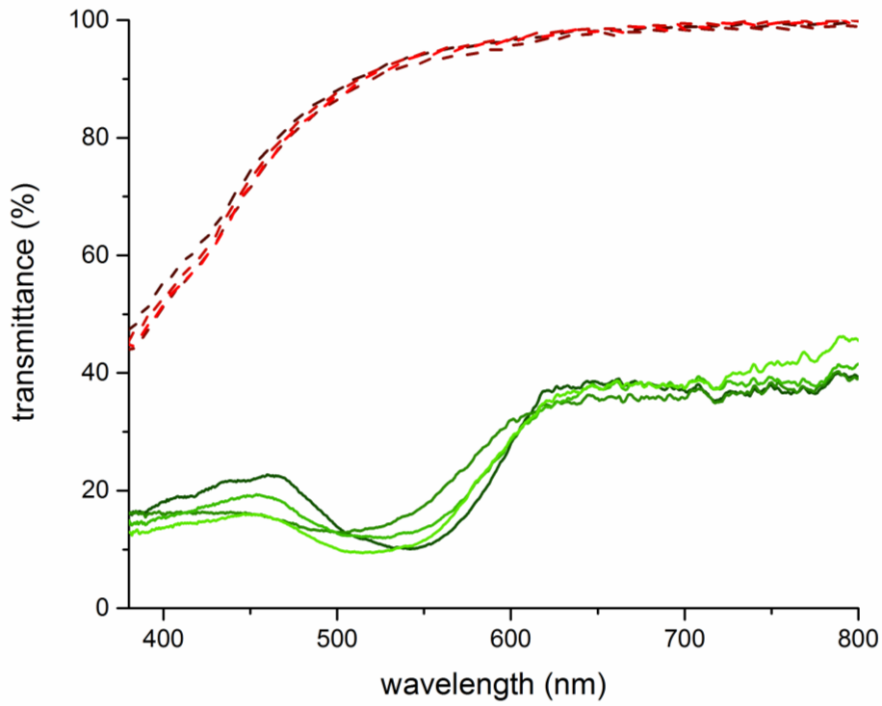

Figure S1: Transmittance spectra of single wing scales in air (solid lines) and immersed in a refractive index fluid with n = 1.55 (dashed lines). The strong absorption at UV wavelengths indicates the presence of a wavelength-selective absorbing pigment. The transmittance through at ~540 nm for the air-immersed scales show the photonic response of the nanostructure present in the scales (Figure 2).

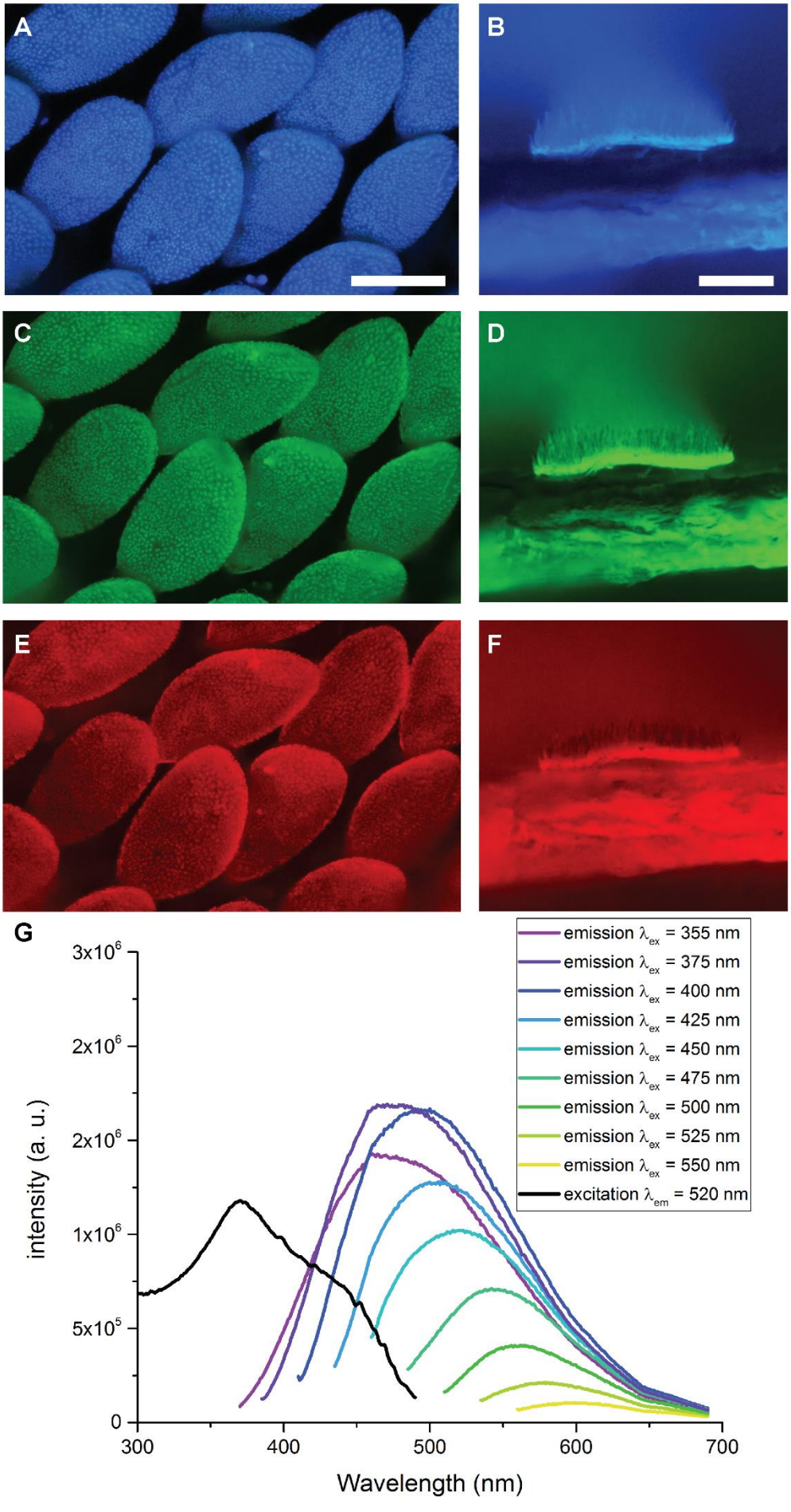

Figure S2: Fluorescence microscopy of *H. argentea* scales in (A,C,E) top-view and (B,D,F) for the cross-section of a single scale. The different panels show (A,B) UV-induced blue fluorescence (excitation 330-380 nm / cut-off 420 nm), (C,D) blue-induced green fluorescence (excitation 450-480 nm / cut-off 515 nm), and (E,F) green-induced red fluorescence channel (excitation 510-550 nm / cut-off 590 nm), respectively. Scale bars: (A,C,E) 50 um, (B,D,F) 20 um. (G) Spectrofluorimetric characterisation. The emission (colour solid lines) and the excitation (black solid line) of the sample are plotted. For emission measurements, the excitation wavelength was varied from 355 to 550 nm. The excitation measurement was carried out with a fixed emission wavelength of 520 nm.

Figure S3: Different *Hoplia argentea* specimen with different degrees of missing scales, resulting in a shift from the green to brown colour. Scale bar: 2 mm.

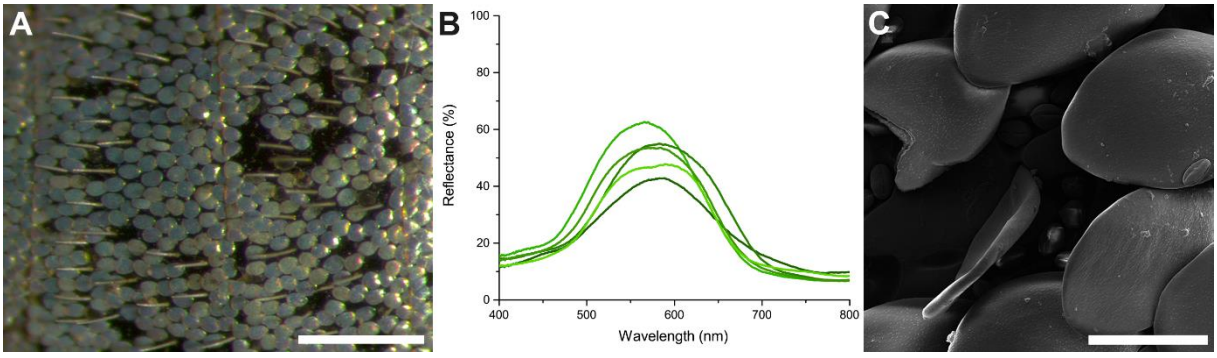

Figure S4: (A) Ventral side of *Hoplia argentea*. (B) Reflectance spectra of scales from the ventral side. (C) SEM of the ventral side scales. We note the absence of filaments. Scale bars: (A) 500 µm, (C) 50 µm.